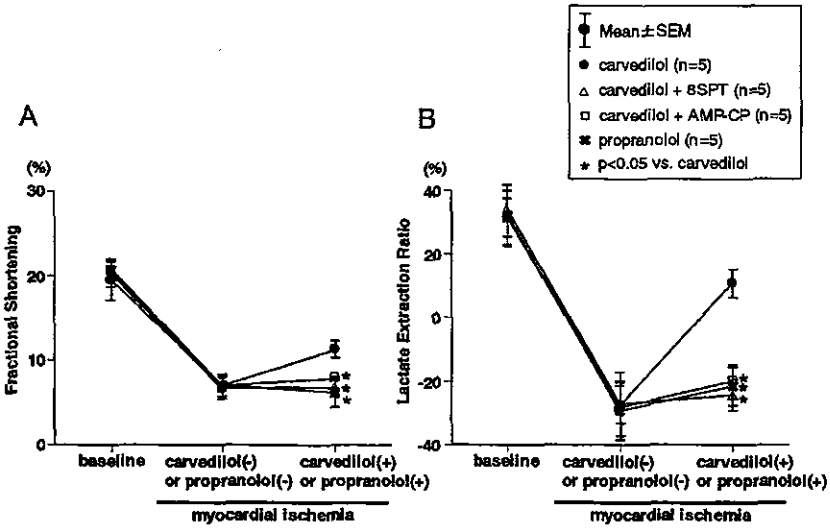

Figure 3. Changes of FS (A) and LER (B) in ischemic myocardium. Statistical analysis was performed by ANOVA followed by Bonferroni's test.

constant low-CPP state, suggesting that myocardial ischemia was improved by carvedilol. These effects of carvedilol were blunted by administration of either 8-SPT or AMP-CP. Unlike carvedilol, an infusion of propranolol did not alter VAD(Ado), CBF, LER, or FS (Figures 1 through 3).

Reduction of Oxidative Stress and Beneficial Effect of Carvedilol in Ischemic Myocardium

In 5 dogs, reduction of CBF caused an increase of VAD(8-Iso-$F_{2\alpha}$), which was reduced by carvedilol (Figure 4A through 4C). Under these conditions, VAD(Ado) was increased by infusion of carvedilol (Figure 4D). In another 5 dogs, an infusion of SOD did not change either hemodynamic parameters or VAD(8-Iso-$F_{2\alpha}$) at nonischemic baseline conditions (Figure 4A through 4C). After the reduction of CBF to 50%, VAD(Ado) increased to the level seen in the presence of carvedilol without SOD (Figure 4D), whereas VAD(8-Iso-$F_{2\alpha}$) did not increase (Figure 4C). Addition of carvedilol did not further attenuate VAD(8-Iso-$F_{2\alpha}$) or increase VAD(Ado) (Figure 4C and 4D).

Effects of Carvedilol on Infarct Size

Seven of 64 dogs were excluded from analysis because their subendocardial collateral flow was >15 mL · 100 g^{-1} · min^{-1}, so 57 dogs completed the protocol satisfactorily. Among these 57 dogs, 18 dogs developed ventricular fibrillation at least once, and ventricular fibrillation that matched the exclusion criteria occurred in 15 dogs, so these animals were also excluded from analysis. The numbers of the dogs that met the exclusion criteria of ventricular fibrillation were 2, 2, 0, 2, 3, 3, and 3 in the saline, the DMSO, the carvedilol, the carvedilol+8-SPT, the carvedilol+AMP-CP, the 8-SPT, and the AMP-CP groups, respectively.

Neither aortic blood pressure (≈104 mm Hg) nor heart rate (≈136 min^{-1}) showed any differences among the 7 groups throughout the protocol. The Table shows the area at risk and the endocardial collateral blood flow in the LAD region during myocardial ischemia. There were no significant differences in the area at risk and collateral flow among the 7 groups during myocardial ischemia (Table). Figure 5 shows

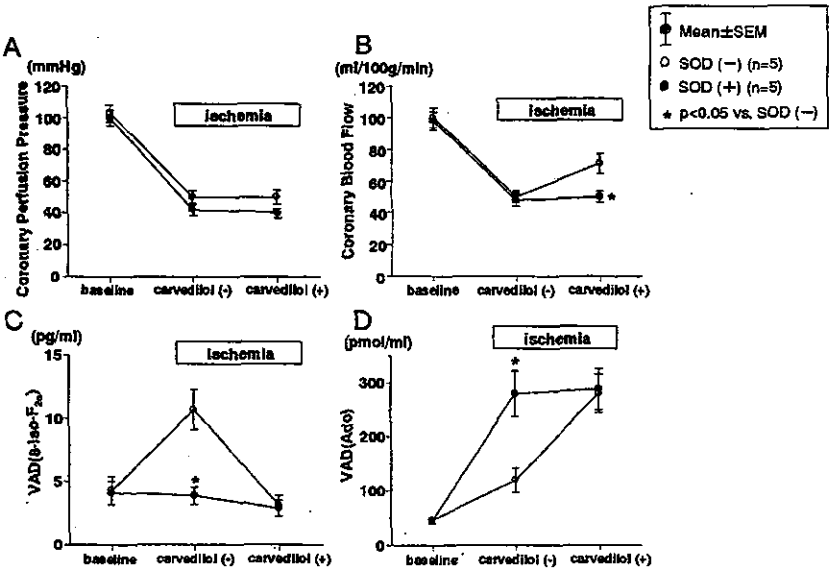

Figure 4. Changes of CPP (A), CBF (B), VAD(8-Iso-$F_{2\alpha}$) (C), and VAD(Ado) (D) in ischemic myocardium. Statistical significance was tested by ANOVA followed by Bonferroni's test.

Area at Risk and Collateral Blood Flow During Myocardial Ischemia in Each Group

Groups	Risk Area, %	CBF During Myocardial Ischemia, mL·100 g^{-1}·min^{-1}
1. Control (saline) group	38.9±1.2	7.8±1.3
2. DMSO group	40.2±1.5	8.1±2.3
3. Carvedilol group	41.5±2.2	8.0±2.6
4. Carvedilol group+8-SPT group	39.3±3.3	9.0±2.0
5. Carvedilol group+AMP-CP group	40.9±3.3	8.7±1.9
6. 8-SPT group	43.1±1.9	8.3±1.9
7. AMP-CP group	41.2±2.1	8.2±1.5

Values are expressed as mean±SEM. There were no differences in the area at risk and collateral blood flow in all of the groups. Statistical significance was tested by ANOVA, followed by Bonferroni's test.

that carvedilol decreased infarct size compared with the control groups. This protective effect was completely blocked by either 8-SPT or AMP-CP, suggesting that the reduction of infarct size by carvedilol was attributable to an adenosine-dependent mechanism.

Effect of Carvedilol on Ecto-5′-Nucleotidase Activity in HUVECs

In HUVECs, carvedilol increased ecto-5′-nucleotidase activity by 35.4±8.4% ($P<0.01$) (Figure 6A). Exposure to xanthine and xanthine oxidase decreased ecto-5′-nucleotidase activity, whereas concomitant addition of carvedilol restored ecto-5′-nucleotidase activity to 104.9±8.7% of the baseline levels ($P<0.01$) (Figure 6B). Neither carvedilol nor xanthine and xanthine oxidase had any effect on cytosolic 5′-nucleotidase.

Discussion

In the present study, we demonstrated that carvedilol increases both adenosine release and CBF in ischemic and nonischemic hearts via reduction of oxidative stress and restoration of ecto-5′-nucleotidase activity. We also showed that carvedilol could limit infarct size and that this effect was attributable to the reduction of oxidative stress and an adenosine- or ecto-5′-nucleotidase–dependent mechanism. These findings suggested that the cardioprotective effect of carvedilol was attributable to an increase of adenosine in ischemic myocardium in addition to its β-blocking action, because propranolol did not mimic this effect.

Influence of Carvedilol on Adenosine Release in Ischemic Hearts

The β-adrenoreceptors in coronary smooth muscle are involved in coronary vasodilation, and their stimulation is thought to increase CBF via the relaxation of vascular smooth muscle and increased myocardial oxygen demand. Therefore, it may seem unusual that a β-blocker like carvedilol would cause coronary vasodilation. There are several possible explanations for the present findings. First, carvedilol itself may cause vasodilation separately from its β-blocking activity. Indeed, although carvedilol does not have a nitroxy moiety, its chemical structure predicts that the drug could also block α_1-adrenoceptors,[20] which would cause vasodilation. We cannot exclude this possibility, but the role of α_1-adrenoceptor blockade in the vasodilatory effect of carvedilol seems likely to be minor, because we have previously reported that blockade of α_1-adrenoceptors attenuates adenosine release in ischemic myocardium,[21] whereas we found that carvedilol caused an increase of adenosine production. Second, carvedilol may increase vasodilatory substances such as NO or adenosine. We demonstrated that carvedilol could increase cardiac adenosine production independently of its β-blocking effect in the present study, because propranolol did not increase CBF under the same circumstances (Figures 1 through 3). Intriguingly, the carvedilol-induced increases in both adenosine release and coronary vasodilation were greater in ischemic heart than in nonischemic heart. There was a significant difference between the influence of carvedilol on coronary vasodilation under nonischemic and ischemic conditions in the present study, because the percent

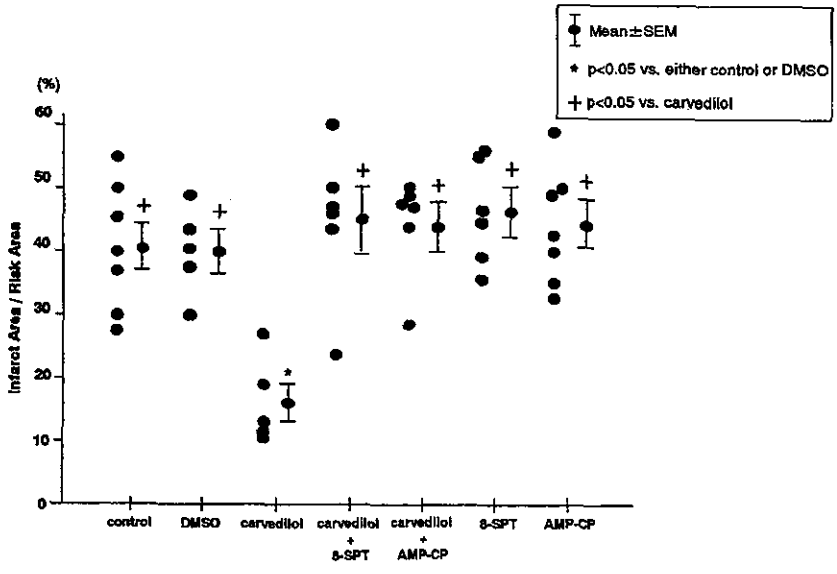

Figure 5. Infarct size as a percentage of area at risk. Infarct size was decreased in carvedilol group compared with control group, and this improvement was blocked by either 8-SPT or AMP-CP. *Statistical significance* was tested by ANOVA followed by Bonferroni's test.

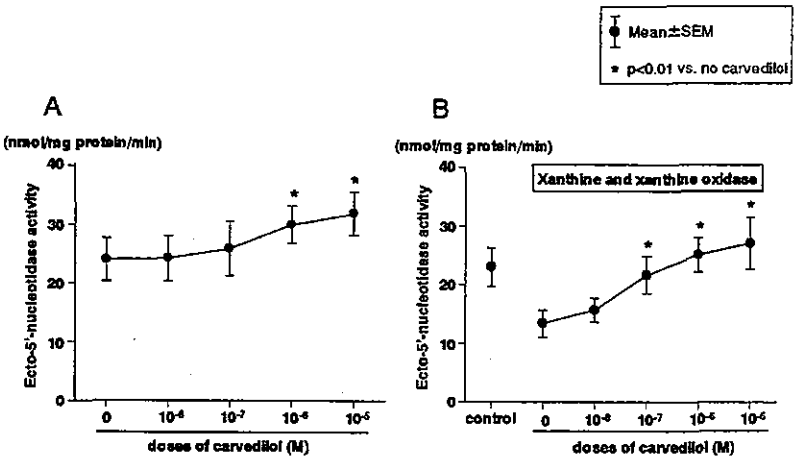

Figure 6. Ecto-5′-nucleotidase activity of HUVECs in presence or absence of carvedilol or xanthine and xanthine oxidase. Statistical significance was tested by ANOVA followed by Bonferroni's test.

increases of CBF in nonischemic and ischemic myocardium were 14.4±1.1% and 50.6±10.1% ($P<0.05$), respectively. One possible explanation is that carvedilol may bind more tightly to β-adrenoreceptors under ischemic conditions than nonischemic conditions, and β-adrenoreceptors are also upregulated in the ischemic heart,[22] which may enhance the adenosine-producing effect of carvedilol. Alternatively, even if carvedilol decreases coronary artery tone in nonischemic heart as well as ischemic heart, the activity of other endogenous vasodilators may decrease to maintain coronary autoregulation. Conversely, the effects of other vasodilators may already be maximal in ischemic hearts, so that carvedilol-induced adenosine release becomes a major determinant of coronary artery tone when adenosine-dependent coronary vasodilation is submaximal. A third possibility is that carvedilol may reduce the levels of substances that attenuate adenosine release and are increased in ischemic myocardium. Because carvedilol is reported to decrease oxidative stress and such stress reduces adenosine production, antioxidant activity of carvedilol may be involved in adenosine-dependent coronary vasodilation and cardioprotection. We showed such evidence in the present study.

In this context, several lines of evidence support the concept that adenosine can markedly attenuate ischemia/reperfusion injury,[12,23] and we suggest that carvedilol-induced adenosine release is important for cardioprotection.

Mechanism of the Carvedilol-Induced Increase of Cardiac Adenosine

In ischemic hearts, carvedilol caused reduction of oxidative stress and increases in both adenosine release and CBF. Also, in HUVECs under oxidative stress, carvedilol restored ecto-5′-nucleotidase activity to the control level. These findings suggest that carvedilol may eliminate the factors that impaired ecto-5′-nucleotidase activity under ischemic conditions. Oxidative stress is one of these factors. Because oxygen-derived free radicals attenuate the ischemia-induced activation of ecto-5′-nucleotidase, elimination of oxidative stress may increase adenosine release in the ischemic myocardium. We observed that carvedilol could reduce oxidative stress, so this action may explain the present findings. Because ecto-5′-nucleotidase is susceptible to impairment by oxygen-derived free radicals, it is likely that the beneficial effect of carvedilol on myocardial ischemia in the present study was attributable to its antioxidant activity.

Clinical Relevance and Limitations

Carvedilol has been shown to be effective for treating heart failure.[5] Its effective clinical dose is about 0.1 to 0.2 μg/mL, and the calculated cardiac concentration of carvedilol in the present study is ≈1 μg/mL. In dogs, carvedilol at 1 and 4 μg/mL decreased blood pressure by 9% and 32%, respectively (data not shown), suggesting that the concentration of 1 μg/mL of carvedilol in canine heats was comparable to a clinical dose of carvedilol. This difference may be also attributable to species differences, the route of administration of carvedilol, or conscious/anesthetic conditions.

The present study hinted that the mechanism by which carvedilol potently ameliorates heart failure, especially ischemic heart failure, may be related to adenosine.[12] Carvedilol may have the ability to both antagonize β-adrenoceptors and increase adenosine release.

Tumor necrosis factor-α is inhibited by both carvedilol and adenosine[24,25] and has been indicated to have a role in the pathology of congestive heart failure. Because the present study hints that the cardioprotection afforded by carvedilol is adenosine-dependent, it follows that the clinical effects of carvedilol may also be adenosine-dependent. If this hypothesis receives further validation, adenosine and potentiators of adenosine production or adenosine receptor agonists may become candidates for the treatment of heart failure.

Acknowledgments

This study was supported by Grants-in-aid for Scientific Research 12470153 and 12877107 from the Japanese Ministry of Education, Culture, Sports, Science, and Technology; a Health and Labor Sciences Research Grant for Human Genome, Tissue Engineering, and Food Biotechnology (H13-Genome-011); and a Health and Labor Sciences Research Grant for Comprehensive Research on Aging and Health (H13-21seiki(seikatsu)-23, H14Tokushitsu-38) from the Japanese Ministry of Health and Labor and Welfare. The authors gratefully acknowledge the technical assistance of Tomi Fukushima and Junko Yamada during the conduct of the experiments.

References

1. Saxenhofer H, Morger D, Weidmann P, et al. Modulation of noradrenergic but not angiotensinergic blood pressure control by beta-blockade with carteolol. *J Hypertens.* 1991;9:1049–1056.
2. Silke B, Verma SP, Hussain M, et al. Haemodynamic dose-response effects of i.v. penbutolol in angina pectoris. *Br J Clin Pharmacol.* 1983; 16:529–535.
3. Packer M, Coats AJ, Fowler MB, et al. Effect of carvedilol on survival in severe chronic heart failure. *N Engl J Med.* 2001;344:1651–1658.
4. Dargie HJ. Effect of carvedilol on outcome after myocardial infarction in patients with left-ventricular dysfunction: the CAPRICORN randomised trial. *Lancet.* 2001;357:1385–1390.
5. Metra M, Nardi M, Giubbini R, et al. Effects of short- and long-term carvedilol administration on rest and exercise hemodynamic variables, exercise capacity and clinical conditions in patients with idiopathic dilated cardiomyopathy. *J Am Coll Cardiol.* 1994;24:1678–1687.
6. Ruffolo RR Jr, Gellai M, Hieble JP, et al. The pharmacology of carvedilol. *Eur J Clin Pharmacol.* 1990;38(suppl 2):S82–S88.
7. Gretzer I, Hjemdahl P. Differences between the effects of metoprolol and prazosin on the forearm vasculature in primary hypertension. *J Hypertens.* 1997;15:1317–1326.
8. Oettl K, Greilberger J, Zangger K, et al. Radical-scavenging and iron-chelating properties of carvedilol, an antihypertensive drug with antioxidative activity. *Biochem Pharmacol.* 2001;62:241–248.
9. Huang WH, Wang Y, Askari A. (Na+/K+)-ATPase: inactivation and degradation induced by oxygen radicals. *Int J Biochem.* 1992;24: 621–626.
10. Guerra L, Cerbai E, Gessi S, et al. The effect of oxygen free radicals on calcium current and dihydropyridine binding sites in guinea pig ventricular myocytes. *Br J Pharmacol.* 1996;118:1278–1284.
11. Kitakaze M, Hori M, Takashima S, et al. Superoxide dismutase enhances ischemia-induced reactive hyperemic flow and adenosine release in dogs: a role of 5′-nucleotidase activity. *Circ Res.* 1992;71:558–566.
12. Kitakaze M, Minamino T, Node K, et al. Adenosine and cardioprotection in the diseased heart. *Jpn Circ J.* 1999;63:231–243.
13. Kitakaze M, Minamino T, Node K, et al. Beneficial effects of inhibition of angiotensin-converting enzyme on ischemic myocardium during coronary hypoperfusion in dogs. *Circulation.* 1995;92:950–961.
14. Bergmeyer HU. *Methods of Enzymatic Analysis.* 1st ed. New York, NY: Academic Press Inc; 1963:266–270.
15. Smith K, Varon HH, Race GJ, et al. Serum 5′-nucleotidase in patients with tumor in the liver. *Cancer.* 1965;19:1281–1285.
16. Kitakaze M, Hori M, Morioka T, et al. Alpha1-adrenoceptor activation mediates the infarct size limiting effect of ischemic preconditioning through augmentation of 5′-nucleotidase activity and adenosine release. *J Clin Invest.* 1994;93:2197–2205.
17. Mori H, Haruyama S, Shinozaki Y, et al. New nonradioactive microspheres and more sensitive X-ray fluorescence to measure regional blood flow. *Am J Physiol.* 1992;263:H1946–H1957.
18. Snedecor GW, Cochran WG. *Statistical Methods.* Ames, Iowa: Iowa State University Press; 1972:258–298.
19. Steel RGD, Torrie JH. *Principles and Procedures of Statistics: A Biomedical Approach.* 2nd ed. New York, NY: McGraw-Hill Publishing Co; 1980:137–238.
20. Feuerstein GZ, Ruffolo RR Jr. Carvedilol, a novel multiple action antihypertensive agent with antioxidant activity and the potential for myocardial and vascular protection. *Eur Heart J.* 1995;16(suppl F):38–42.
21. Kitakaze M, Hori M, Tamai J, et al. α_1-Adrenoceptor activity regulates release of adenosine from the ischemic myocardium in dogs. *Circ Res.* 1987;60:631–639.
22. Brodde OE, Zerkowski HR, Borst HG, et al. Drug- and disease-induced changes of human cardiac beta 1- and beta 2-adrenoceptors. *Eur Heart J.* 1989;10(suppl B):38–44.
23. Babbitt TG, Virmani R, Norton R Jr, et al. Adenosine administration during reperfusion after 3 hours of ischemia: effects on infarct size, ventricular function, and regional myocardial blood flow. *Am Heart J.* 1990;120:808–818.
24. Parmely MJ, Zhou WW, Edwards CK, et al. Adenosine and a related carbocyclic nucleoside analogue selectively inhibit tumor necrosis factor-α production and protect mice against endotoxin challenge. *J Immunol.* 1993;151:389–396.
25. Rossig L, Haendeler J, Mallat Z, et al. Congestive heart failure induces endothelial cell apoptosis: protective role of carvedilol. *J Am Coll Cardiol.* 2000;36:2081–2089.

Methotrexate and MX-68, a New Derivative of Methotrexate, Limit Infarct Size via Adenosine-Dependent Mechanisms in Canine Hearts

Hiroshi Asanuma, MD, PhD, Shoji Sanada, MD, PhD,* Akiko Ogai, BS,† Tetsuo Minamino, MD, PhD,* Seiji Takashima, MD, PhD,* Masanori Asakura, MD, PhD,* Hisakazu Ogita, MD, PhD,* Yoshiro Shinozaki, BS,‡ Hidezo Mori, MD, PhD,† Koichi Node, MD, PhD,§ Hitonobu Tomoike, MD, PhD,† Masatsugu Hori, MD, PhD,* and Masafumi Kitakaze, MD, PhD†*

Abstract: Methotrexate, an anti-rheumatic agent, has recently been reported to show an anti-inflammatory action via ecto-5′-nucleotidase- and adenosine-dependent mechanisms. Because ecto-5′-nucleotidase contributes to the production of adenosine and adenosine has a potent cardioprotective effect against ischemia/reperfusion injury, we investigated whether methotrexate or MX-68 [N-1-((2,4-diamino-6-pteridinyl) methyl)-3,4-dihydro-2H-1,4-benzothiazine-7- carbonyl]-N-2- aminoadipic acid] could reduce infarct size via adenosine-dependent mechanisms. In beagle dogs, the left anterior descending coronary artery was perfused through a bypass tube, which was occluded for 90 minutes followed by 6 hours of reperfusion. The size of infarcts was assessed by TTC staining. MX-68 reduced infarct size compared with that in untreated dogs (13.7 ± 1.9 versus 38.6 ± 5.3%, $P < 0.01$). This effect was completely blunted by either the adenosine receptor antagonist 8-sulfophenyltheophylline (8-SPT) (45.0 ± 4.6% and 46.8 ± 5.8% in the 8-SPT and MX-68 + 8-SPT groups, respectively) or by the ecto-5′-nucleotidase inhibitor α,β-methylenadenosine 5′-diphosphate (AMP-CP) (44.0 ± 4.5% and 46.7 ± 5.8% in the AMP-CP and MX-68 + AMP-CP groups, respectively). Methotrexate also reduced infarct size to a level comparable with that in the MX-68 group, and its effect was also blunted by 8-SPT. There were no significant differences of collateral blood flow or risk area between the groups. We conclude that methotrexate and its derivative (MX-68) both limit infarct size via adenosine-dependent mechanisms.

Received for publication August 31, 2003; accepted January 14, 2004.

From the *Department of Internal Medicine and Therapeutics, Osaka University Graduate School of Medicine, Suita; †Division of Cardiology, National Cardiovascular Center, Suita; ‡Department of Physiological Science, Tokai University School of Medicine, Isehara; and §Cardiovascular Division, Saga University School of Medicine, Saga, Japan.

Supported in part by Grants-in-aid for Scientific Research (No. 12470153 and 12877107) from the Ministry of Education, Science, Sports, and Culture, Japan, and the Smoking Research Foundation in Japan.

Reprints: Masafumi Kitakaze, MD, PhD, Division of Cardiology, National Cardiovascular Center, Suita, Japan 5-7-1 Fujishirodai, Suita, Osaka 565-8565, Japan (e-mail: kitakaze@zf6.so-net.ne.jp).

Key Words: adenosine, ischemia, infarction, inflammation, methotrexate, ecto-5′-nucleotidase, heart

(*J Cardiovasc Pharmacol*™ 2004;43:574–579)

Although the limitation of infarct size is an important strategy to overcome ischemic heart failure,[1,2] which is one of the major causes of death today, the most effective adjunctive therapy for ischemic heart disease remains unclear.[3] The infarct size-limiting effects of many drugs with anti-inflammatory actions has been tested in an attempt to find effective treatments for myocardial infarction,[4,9] because the pathophysiology of ischemia/reperfusion injury resembles that of inflammation, including such features as leukocyte infiltration and cytokine production. However, the effect of anti-inflammatory drugs on infarct size seems to vary. Some studies have shown that steroids are effective at reducing infarct size and preventing cardiac remodeling.[7,8] However, other reports have suggested that steroids cannot reduce infarct size[9] and these drugs have even been suggested to exacerbate myocardial ischemic injury.[4,6] On the other hand, other anti-inflammatory agents such as statin and estrogen seem to have a cardioprotective effect.[10,12] Therefore, attenuation of inflammation does not necessarily have a protective effect against ischemia/reperfusion injury, but has the possibility of mediating cardioprotection. Interestingly, the anti-inflammatory effect of methotrexate (MTX) has been demonstrated to be mediated via adenosine- and ecto-5′-nucleotidase-dependent mechanisms both in vitro and in vivo.[13] Adenosine inhibits the activation of leukocytes and platelets and also decreases cytokine production.[14,16] Adenosine has recently been recognized to show a cardioprotective effect against ischemia/reperfusion injury.[17,18] MTX promotes adenosine release by a variety of different cells and tissues, particularly in the presence of physiological stress. After MTX is taken up by cells, MTX or its metabolites inhibit 5-aminoimidazole-4-

carboxamide ribonucleotide (AICAR) transformylase, leading to an increase of the AICAR level. We have previously reported that AICAR activates ecto-5′-nucleotidase in the myocardium and increases adenosine release, which may limit infarct size.[19] These reports suggest that MTX, a potent anti-inflammatory agent, may prevent ischemia/reperfusion injury via adenosine-dependent mechanisms.

To test this hypothesis, we examined whether MTX or a new MTX derivative, N-1-((2,4-diamino-6-pteridinyl) methyl)-3,4- dihydro-2H-1, 4-benzothiazine-7-carbonyl)-N-2-aminoadipic acid[20] (MX-68) could limit infarct size via adenosine- or ecto-5′-nucleotidase-dependent mechanisms.

MATERIALS AND METHODS

Instrumentation

Beagle dogs weighing 10 to 13 kg were anesthetized with pentobarbital sodium (30 mg kg^{-1}, iv). The experimental setup was reported previously.[21] After opening the chest and administration of heparin (500 U kg^{-1}, iv), the left anterior descending coronary artery (LAD) was cannulated for perfusion with blood from the left carotid artery through an extracorporeal bypass tube, and the aortic blood pressure was monitored in this tube. Another cannula was placed in the left atrium for injection of microspheres to measure collateral blood flow during coronary occlusion. The baseline pH, PO_2, and PCO_2 of systemic arterial blood were 7.40 ± 0.02, 106 ± 3 mm Hg, and 38.5 ± 2.0 mm Hg, respectively.

All studies conformed to the "Position of the American Heart Association on Research Animal Use", as adopted by the Association in November 1984.

Experimental Protocols

The systolic and diastolic aortic blood pressures and the heart rate were monitored as hemodynamic parameters.

After hemodynamics became stable, coronary arterial and venous blood samples were obtained for blood gas analysis. In the control group (n = 7), the bypass tube to the LAD was occluded for 90 minutes, followed by 6 hours of reperfusion with infusion of the vehicle (PBS) from 15 minutes before bypass occlusion until the end of reperfusion (except during bypass occlusion). Hemodynamic parameters were monitored during myocardial ischemia and after the start of reperfusion. In the MX-68 group (n = 6), MX-68 dissolved in PBS was infused as a bolus (0.1 mg kg^{-1}) and then infused continuously (0.1 mg kg^{-1} h^{-1}) into a systemic vein from 10 minutes before bypass occlusion until the end of the 6-hour reperfusion period (except during bypass occlusion). The effect of MX-68 was also tested during intracoronary infusion of either 8-sulfophenyltheophylline (8-SPT, 50 μg kg^{-1} min^{-1}) or α,β-methylenadenosine 5′-diphosphate (AMP-CP, 30 μg kg^{-1} min^{-1}) from 15 minutes before bypass occlusion until 6 hours of reperfusion (except during bypass occlusion) in the MX-68+8-SPT group (n = 5) and the MX-68+AMP-CP group (n = 5), respectively. In the MTX group (n = 5), MTX was given as an intravenous bolus (0.05 mg kg^{-1}) and then as a continuous infusion (0.05 mg kg^{-1} h^{-1}) according to the same schedule as that for MX-68. In the MTX+8-SPT group (n = 5), 8-SPT and MTX were administered by the same schedule as for the MX-68+8-SPT group. We also tested whether MX-68 was effective after the onset of reperfusion (the MX-68 (post) group); MX-68 was given as a bolus infusion (0.1 mg kg^{-1}) into a systemic vein at the start of reperfusion and then as a continuous infusion (0.1 mg kg^{-1} h^{-1}) for 6 hours (n = 7). In all of these groups, the bypass tube was occluded for 90 minutes, followed by 6 hours of reperfusion, and the infarct size was assessed at 6 hours as reported previously.[21] Microspheres were infused at 45 minutes after the onset of coronary occlusion to measure collateral blood flow.

Measurement of Regional Blood Flow

Regional myocardial blood flow was determined by the microsphere technique as described previously.[21] Microspheres (Sekisui Plastic Co., Ltd., Tokyo, Japan) made of an inert plastic were labeled with bromine (Br). The mean diameter of the microspheres was 15 μm and the specific gravity was 1.34 for Br. The microspheres were suspended in isotonic saline with 0.01% Tween 80 to prevent aggregation, and were sonicated for 5 minutes followed by vortexing for 5 minutes immediately before injection. Just before administration of the microspheres, a reference blood sample was withdrawn from the femoral artery at a constant rate of 8 mL/min for 2 minutes. Approximately 1 mL of the microsphere suspension (2 to 4 × 10^6 microspheres) was injected into the left atrium, and then was flushed with warm (37°C) saline (5 mL). Microspheres were administered 80 minutes after occlusion of the bypass tube.

The radiograph fluorescent activity of the stable heavy element was measured with a wavelength dispersive spectrometer (PW 1480, Phillips Co., Ltd., Almelo, The Netherlands). The microspheres were irradiated by a primary radiograph beam, causing electrons to fall back to a lower orbit and emit measurable energy. Because the energy emitted is characteristic of a specific element, it is possible to quantify the radiograph fluorescence of any heavy element with which the microspheres are labeled. Myocardial blood flow was calculated according to the following formula: Flow = (Tissue count) × (Reference flow)/(Reference count), and was expressed as milliliters per minute per gram wet weight. Endomyocardial blood flow was measured in the inner half of the left ventricular (LV) wall.

Measurement of Infarct Size

After reperfusion for 6 hours, the LAD was reoccluded and perfused with autologous blood. Evans blue dye was in-

jected into a systemic vein to identify the area at risk and the nonischemic area.[21] The heart was then immediately removed and sliced into serial transverse sections that were 6 to 7 mm in width. The nonischemic area was defined as the tissue showing blue staining. The ischemic region was harvested and incubated at 37°C for 20 to 30 minutes in 1% 2,3,5-triphenyltetrazolium chloride (TTC, Sigma Chemical Company) in 0.1 mol/L phosphate buffer adjusted to pH 7.4. TTC stains the noninfarcted myocardium a brick-red color, indicating the presence of a formazan product created through the reduction of TTC by dehydrogenases in viable tissues. The infarct size was expressed as a percentage of the area at risk.

Selection Criteria

To ensure that all of the animals included in analysis of infarct size were healthy and exposed to a similar extent of ischemia, the following criteria were used to exclude unsatisfactory dogs: (1) subendocardial collateral flow > 15 mL 100 g^{-1} min^{-1}, (2) heart rate >170 bpm, and (3) more than 2 consecutive attempts required to convert ventricular fibrillation with low-energy DC pulses applied directly to the heart.

Statistical Analysis

Statistical analysis was performed with ANOVA for comparisons among the groups. If ANOVA indicated a significant difference, paired data were compared using Bonferroni test.[22,23] Changes of the hemodynamic parameters over time were compared by ANOVA with repeated measures. Using endocardial collateral blood flow in the inner half of the LV wall as the covariate, ANCOVA was performed to assess the influence of collateral flow on infarct size. Results are expressed as the mean ± SEM, and $P < 0.05$ was considered significant.

RESULTS

Seventy dogs were randomly assigned to 9 different protocols and the infarct size was determined in each group. Eight dogs were excluded from analysis because subendocardial collateral flow was greater than 15 mL 100 g^{-1} min^{-1}. Among the remaining 62 dogs, 17 developed ventricular fibrillation at least once and fibrillation that fulfilled the exclusion criteria occurred in 9 dogs, which were also excluded from the study.

Mean aortic blood pressure and heart rate (Fig. 1) did not vary among the 9 groups throughout the study. The percent area at risk in the left ventricle and the endocardial collateral blood flow during myocardial ischemia were also not significantly different among the 9 groups (Fig. 2). Figure 3 shows that MX-68 markedly reduced the infarct size compared with that in the control group. This effect of MX-68 was completely

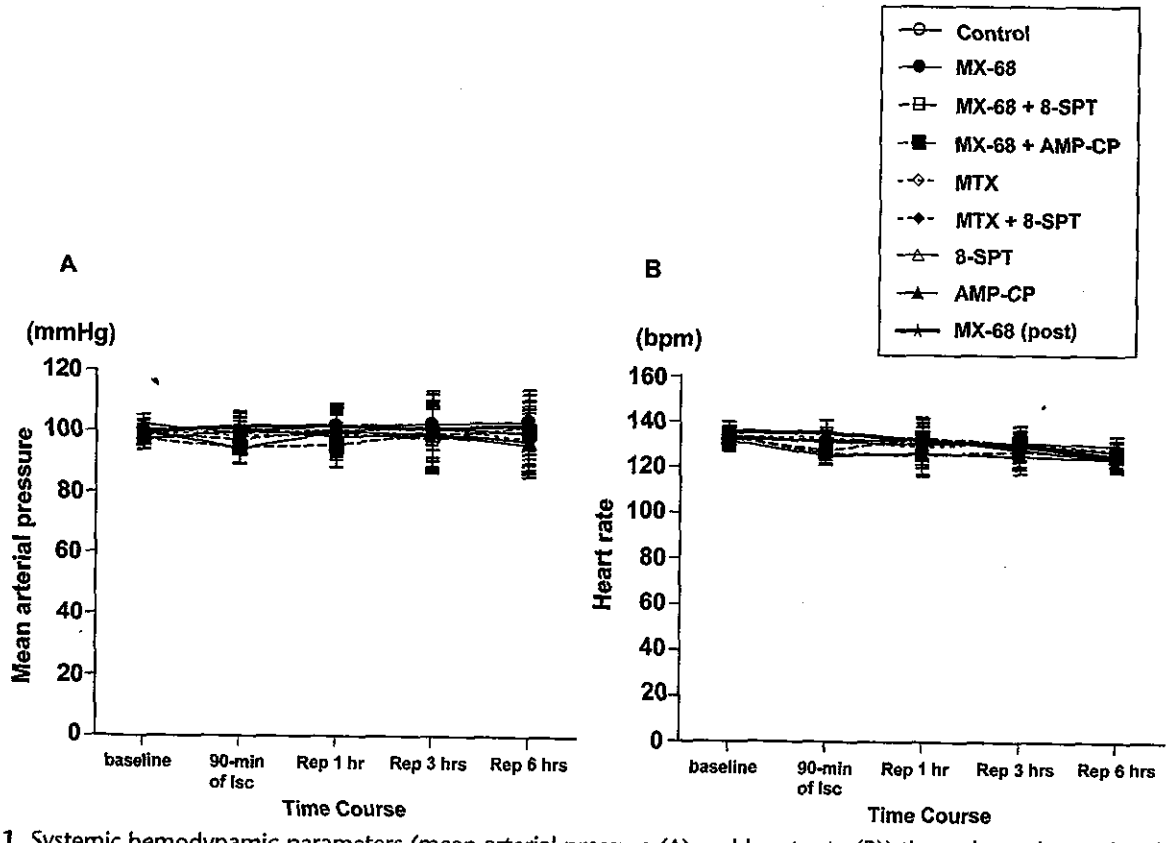

FIGURE 1. Systemic hemodynamic parameters (mean arterial pressure (A) and heart rate (B)) throughout the study. There were no significant changes of these parameters in all the 9 groups. Statistical significance was tested by ANOVA.

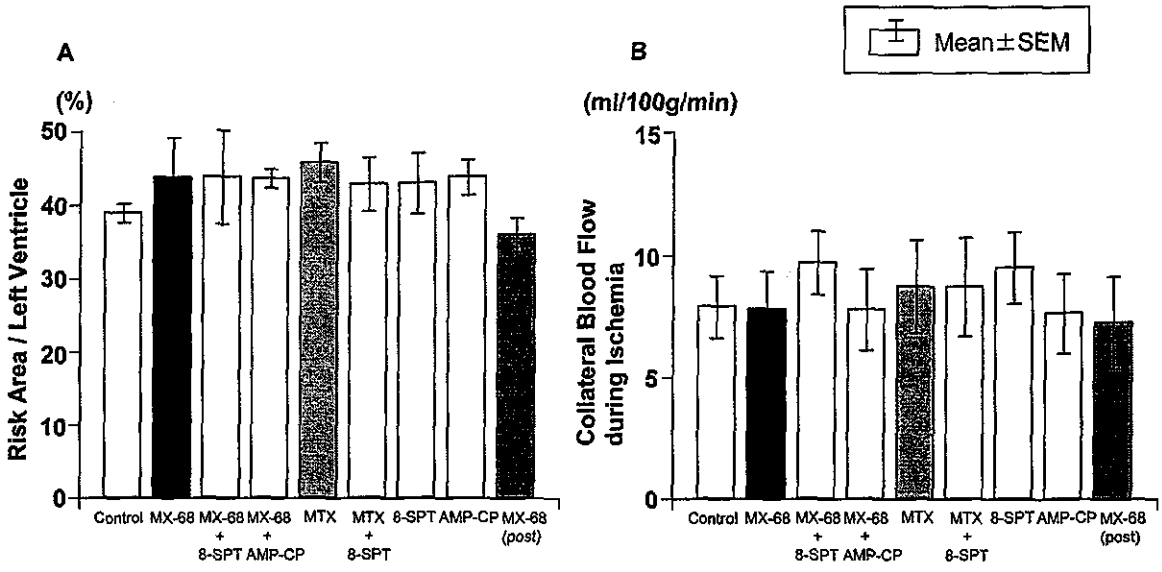

FIGURE 2. Area at risk (A) and collateral blood flow during ischemia (B) in the control group, MTX group, MX-68 group, MTX+8-SPT group, MX-68+8-SPT group, MX-68+AMP-CP group, MX-68(post) group, 8-SPT group, and AMP-CP group. There were no differences of the area at risk and collateral flow during ischemia between these groups. Statistical significance was tested by ANOVA.

blunted by infusion of either 8-SPT or AMP-CP. MTX also reduced infarct size in a similar manner to MX-68, and its protective effect was blunted by 8-SPT. Even when MX-68 was administered after the start of reperfusion, reduction of infarct size was observed to a level between that in the control group and that when MX-68 was administered before ischemia. Regression plots of infarct size versus collateral blood flow are shown in Figure 4, which indicate that the infarct size-limiting effect of either MX-68 or MTX was attributable to an adenosine-dependent mechanism.

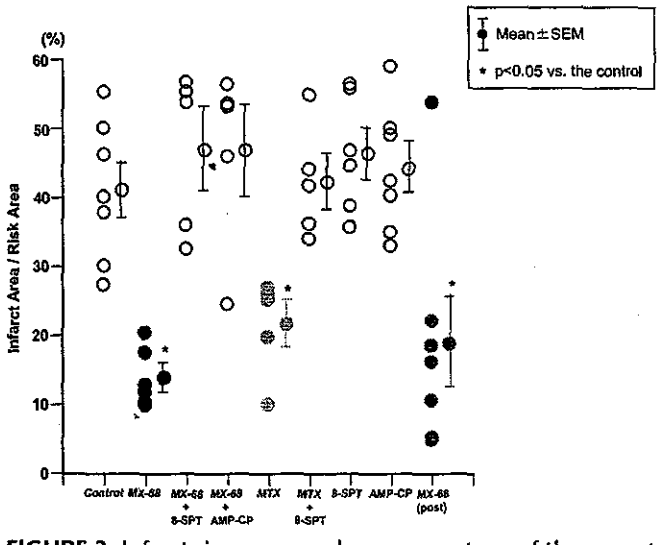

FIGURE 3. Infarct size expressed as a percentage of the area at risk. Infarct size was markedly decreased in the MTX and MX-68 groups compared with the control group, and this improvement was completely reversed by 8-SPT or AMP-CP. Statistical significance was tested by ANOVA.

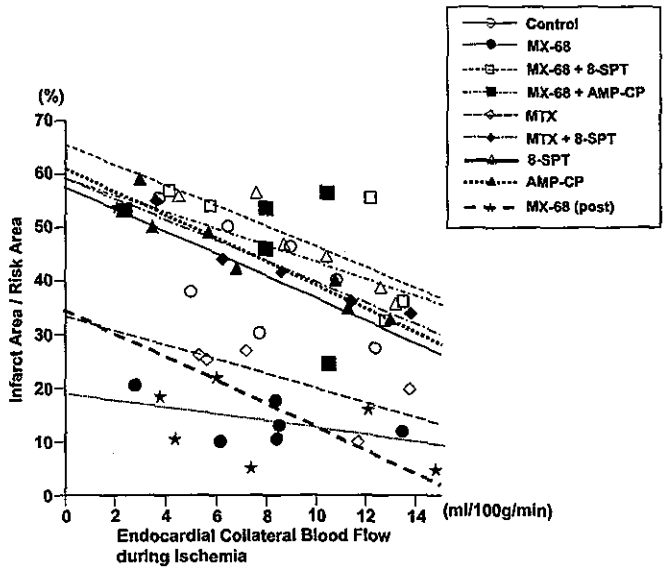

FIGURE 4. Infarct size after 90 minutes of ischemia versus regional collateral flow during ischemia. Infarct size is expressed as a percentage of the area at risk. Infarct size was markedly decreased in the MTX and MX-68 groups compared with the control group. This improvement was completely reversed by 8-SPT or AMP-CP. Statistical significance was tested by ANCOVA.

DISCUSSION

The present study demonstrated that either MTX or MX-68 could markedly reduce infarct size and that the cardioprotective effects of these agents were attributable to ecto-5′-nucleotidase- and adenosine-dependent mechanisms.

Adenosine and the Cardioprotective Effect of MTX or MX-68

Anti-inflammatory drugs such as steroids were thought to have an infarct size-limiting effect[7,8] because the pathophysiology of myocardial infarction resembles tissue inflammation and such drugs can potently ameliorate the tissue inflammatory process. However, steroids and related hormones have been variously reported to decrease infarct size, have no effect, or even increase infarct size.[4,9] On the other hand, other anti-inflammatory agents seem to be effective against ischemia/reperfusion injury. For example, 17β-estradiol is known to have an anti-inflammatory effect[10] and it markedly reduces infarct size.[11] Statins are known to improve vascular inflammation and atherosclerosis, and these drugs also reduce infarct size markedly.[12] Therefore, we cannot necessarily conclude that all anti-inflammatory drugs will be effective for ischemia/reperfusion injury, but we can suggest that these drugs have the possibility of mediating cardioprotection.

MTX and its analog MX-68 are disease-modifying antirheumatic drugs,[20] and their mechanism of action on immune cells was recently reported to be mediated via adenosine.[13] If this is the case in myocardial cells, either MTX or MX-68 would limit infarct size because adenosine markedly reduces the size of infarcts and triggers/mediates the cardioprotective effect of ischemic preconditioning.[24,25] Indeed, the present study revealed that MTX and its analog (MX-68) can ameliorate ischemia/reperfusion injury. We also showed that this action is adenosine-dependent, because the effect of either MTX or MX-68 was blunted by 8-SPT, an adenosine receptor antagonist. Accordingly, both MTX and MX-68 ameliorate ischemia/reperfusion injury via adenosine-related mechanisms.

In immune system cells, the adenosine-related action of MTX was reported to be attributable to ecto-5′-nucleotidase,[13] and this also seems to be the case in the myocardium because the effect of MX-68 and MTX was blunted by an ecto-5′-nucleotidase inhibitor or an adenosine receptor antagonist. Ecto-5′-nucleotidase produces adenosine, and adenosine inhibits norepinephrine release from presynaptic vesicles and attenuates Ca^{2+} influx into myocytes by acting on A_1 receptors and inhibitory G protein.[26,27] Adenosine also increases CBF, inhibits platelet aggregation, and inhibits leukocyte activation via A_2 receptors and stimulatory G protein.[14,16] Since factors such as an increase of norepinephrine, Ca^{2+} overload, decreased CBF, and activation of platelets and leukocytes are deleterious to the heart, control of these factors by adenosine may help to minimize ischemia/reperfusion injury. Several studies have shown that adenosine administration markedly attenuates ischemia/reperfusion injury.[3,15,17]

Role of Adenosine in the Effect of MTX or MX-68

How does MTX or MX-68 act on ecto-5′-nucleotidase? Several possibilities can be suggested. First, activation of ecto-5′-nucleotidase may occur after phosphorylation, as seen with ischemic preconditioning or treatment with phorbol ester, where activation of protein kinase C possibly leads to the phosphorylation and activation of ecto-5′-nucleotidase.[28,29] However, the in vitro activity of myocardial ecto-5′-nucleotidase was not increased by brief exposure to MTX (data not shown), whereas methoxamine and phorbol ester, which phosphorylate and activate ecto-5′-nucleotidase, both activated myocardial ecto-5′-nucleotidase in vitro.[28,29] These results suggest that MTX does not activate ecto-5′-nucleotidase via the process of phosphorylation, so a direct interaction between MTX and the active site of ecto-5′- nucleotidase may be responsible instead.

Second, MTX is reported to increase the tissue level of AICA riboside by inhibition of AICA riboside deaminase,[13] and we have previously shown that AICA riboside increases the activity of ecto-5′-nucleotidase.[19] Therefore, ecto-5′-nucleotidase may be activated when the myocardial AICA riboside is increased during administration of MTX in vivo. However, it has not been clarified how AICA riboside activates ecto-5′-nucleotidase in the heart. Since AICA riboside activates AMP deaminase and inactivates adenosine deaminase, it may also modulate the enzymes related to adenosine metabolism.[30] Accordingly, AICA riboside could increase adenosine production via activation of ecto-5′-nucleotidase, and maintain a high adenosine level by inhibiting enzymes involved in the metabolism of adenosine. In this context, there are many reports that AICA riboside is cardioprotective against ischemia/reperfusion injury via adenosine-dependent mechanisms.[16,30,31]

Clinical Relevance and Limitations

In this study, we demonstrated that both MX-68 and MTX can limit infarct size via adenosine-dependent mechanisms. It would be of interest to test the cardioprotective effect of MTX or MX-68 in the clinical setting of acute myocardial infarction with coronary revascularization, since infusion of adenosine during reperfusion has been shown to limit infarct size.[17] Furthermore, since administration of adenosine can precondition the myocardium prior to sustained ischemia,[24] treatment with MTX or MX-68 may be useful in patients who have coronary artery disease to precondition the myocardium and improve resistance to acute myocardial infarction. However, further studies are necessary to develop either MTX or MX-68 as a drug to treat acute ischemic heart disease.

REFERENCES

1. Resnekov L. The intermediate coronary care unit. A stage in continued coronary care. *Br Heart J.* 1977;39:357–362.
2. Geltman EM, Ehsani AA, Campbell MK, et al. The influence of location and extent of myocardial infarction on long-term ventricular dysrhythmia and mortality. *Circulation.* 1979;60:805–814.
3. Kitakaze M, Hori M. It is time to ask what adenosine can do for cardioprotection (Brief Review). *Heart Vessels.* 1998;13:211–228.
4. Scheuer DA, Mifflin SW. Chronic corticosterone treatment increases myocardial infarct size in rats with ischemia-reperfusion injury. *Am J Physiol.* 1997;272:R2017–R2024.
5. Chapman DW, Skaggs RH, Thomas JR, et al. The effect of cortisone in experimental myocardial infarction. *Am J Med Sci.* 1952;223:41–44.
6. Roberts R, Demello V, Sobel BE. Deleterious effects of methylprednisolone in patients with myocardial infarction. *Circulation.* 1976;53(Suppl I):I204–I206.
7. Braunwald E, Maroko PR. Effects of hyaluronidase and hydrocortisone on myocardial necrosis after coronary occlusion. *Am J Cardiol.* 1976;37:550–556.
8. Shatney CH, MacCarter DJ, Lillehei RC. Temporal factors in the reduction of myocardial infarct volume by methylprednisolone. *Surgery.* 1976;80:61–69.
9. Madias JE, Hood WB Jr. Effects of methylprednisolone on the ischemic damage in patients with acute myocardial infarction. *Circulation.* 1982;65:1106–1113.
10. Squadrito F, Altavilla D, Squadrito G, et al. 17Beta-oestradiol reduces cardiac leukocyte accumulation in myocardial ischaemia reperfusion injury in rat. *Eur J Pharmacol.* 1997;335:185–192.
11. Hale SL, Birnbaum Y, Kloner RA. Beta-Estradiol, but not alpha-estradiol, reduced myocardial necrosis in rabbits after ischemia and reperfusion. *Am Heart J.* 1996;132:258–262.
12. Scalia R, Gooszen ME, Jones SP, et al. Simvastatin exerts both anti-inflammatory and cardioprotective effects in apolipoprotein E-deficient mice. *Circulation.* 2001;103:2598–2603.
13. Babbitt TG, Virmani R, Norton R Jr, et al. Adenosine administration during reperfusion following 3 hours of ischemia: Effects on infarct size, ventricular function, and regional myocardial blood flow. *Am Heart J.* 1990;120:808–818.
14. Dorheim TA, Hoffman A, Van Wylen DGL, et al. Enhanced interstitial fluid adenosine attenuates myocardial stunning. *Surgery.* 1991;110:136–145.
15. Morabito L, Montesinos MC, Schreibman DM, et al. Methotrexate and sulfasalazine promote adenosine release by a mechanism that requires ecto-5′-nucleotidase-mediated conversion of adenine nucleotides. *J Clin Invest.* 1998;101:295–300.
16. Cronstein BN, Levin RI, Belanoff J, et al. Adenosine: an endogenous inhibitor of neutrophil-mediated injury to endothelial cells. *J Clin Invest.* 1986;78:760–770.
17. Kitakaze M, Hori M, Kamada T. The role of adenosine and its interaction with alpha-adrenoceptor activity in myocardial ischemic and reperfusion injury (Brief Review). *Cardiovasc Res.* 1993;27:18–27.
18. Kitakaze M, Minamino T, Node K, et al. Adenosine and cardioprotection in the diseased heart (Brief Review). *Jpn Circ J.* 1999;63:231–243.
19. Hori M, Kitakaze M, Takashima S, et al. AICA riboside improves myocardial ischemia in coronary microembolization in dogs. *Am J Physiol.* 1994;267:H1483–H1495.
20. Mihara M, Urakawa K, Takagi N, et al. In vitro and in vivo biological activities of a novel nonpolyglutamable anti-folate, MX-68. *Immunopharmacology.* 1996;35:41–46.
21. Kitakaze M, Hori M, Morioka T, et al. Alpha$_1$-adrenoceptor activation mediates the infarct size limiting effect of ischemic preconditioning through augmentation of 5′-nucleotidase activity and adenosine release. *J Clin Invest.* 1994;93:2197–2205.
22. Winer BJ. *Statistical Principles in Experimental Design.*2nd ed. New York: McGraw-Hill, Inc.; 1982:1–907.
23. Snedecor GW, Cochran WG. *Statistical Methods.* 6th ed. Ames, Iowa: Iowa State University Press; 1972:258–298.
24. Liu GS, Thornton J, Van Winkle DM, et al. Protection against infarction afforded by preconditioning is mediated by A1 adenosine receptors in rabbit heart. *Circulation.* 1991;84:350–356.
25. Kitakaze M, Hori M, Takashima S, et al. Ischemic preconditioning increases adenosine release and 5′-nucleotidase activity during myocardial ischemia and reperfusion in dogs: Implication for myocardial salvage. *Circulation.* 1993;87:208–215.
26. Richardt G, Wassa W, Kranzhofer R, et al. Adenosine inhibits exocytotic release of endogenous noradrenaline in rat heart: A protective mechanisms in early myocardial ischemia. *Circ Res.* 1987;61:117–123.
27. Sato H, Hori M, Kitakaze M, et al. Endogenous adenosine blunts β-adrenoceptor-mediated inotropic response in hypoperfused canine myocardium. *Circulation.* 1992;85:1594–1603.
28. Kitakaze M, Node K, Minamino T, et al. Role of activation of protein kinase C in the infarct size-limiting effect of ischemic preconditioning through activation of ecto-5′-nucleotidase. *Circulation.* 1996;93:781–791.
29. Kitakaze M, Minamino T, Node K, et al. Activation of ecto-5′-nucleotidase by protein kinase C attenuates irreversible cellular injury due to hypoxia and reoxygenation in rat cardiomyocytes. *J Mol Cell Cardiol.* 1996;28:1945–1955.
30. Gruber HE, Hoffer ME, McAllister DR, et al. Increased adenosine concentration in blood from ischemic myocardium by AICA riboside. Effects on flow, granulocyte, and injury. *Circulation.* 1989;80:1400–1411.
31. Kitakaze M, Takashima S, Minamino T, et al. Improvement by 5-amino-4-imidazole carboxamide riboside of the contractile dysfunction that follows brief periods of ischemia through increases in ecto-5-nucleotidase activity and adenosine release in canine hearts. *Jpn Circ J.* 1999;63:542–553.

Japanese Journal of Applied Physics
Vol. 43, No. 10, 2004, pp. 7324–7328

Quasi-Monochromatic Flash X-Ray Generator Utilizing Disk-Cathode Molybdenum Tube

Eiichi SATO, Michiaki SAGAE, Etsuro TANAKA[1], Yasuomi HAYASI, Rudolf GERMER[2], Hidezo MORI[3], Toshiaki KAWAI[4], Toshio ICHIMARU[5], Shigehiro SATO[6], Kazuyoshi TAKAYAMA[7] and Hideaki IDO[8]

Department of Physics, Iwate Medical University, 3-16-1 Honchodori, Morioka 020-0015, Japan
[1]*Department of Nutritional Science, Faculty of Applied Bio-science, Tokyo University of Agriculture, 1-1-1 Sakuragaoka, Setagaya-ku 156-8502, Japan*
[2]*ITP, FHTW FB1 and TU-Berlin, Blankenhainer Str. 9, D 12249 Berlin, Germany*
[3]*Department of Cardiac Physiology, National Cardiovascular Center Research Institute, 5-7-1 Fujishiro-dai, Suita, Osaka 565-8565, Japan*
[4]*Electron Tube Division #2, Hamamatsu Photonics Inc., 314-5 Shimokanzo, Toyooka Village, Iwata-gun 438-0193, Japan*
[5]*Department of Radiological Technology, School of Health Sciences, Hirosaki University, 66-1 Honcho, Hirosaki 036-8564, Japan*
[6]*Department of Microbiology, School of Medicine, Iwate Medical University, 19-1 Uchimaru, Morioka 020-8505, Japan*
[7]*Shock Wave Research Center, Institute of Fluid Science, Tohoku University, 2-1-1 Katahira, Aoba-ku, Sendai 980-8577, Japan*
[8]*Department of Applied Physics and Informatics, Faculty of Engineering, Tohoku Gakuin University, 1-13-1 Chuo, Tagajo 985-8537, Japan*

(Received April 2, 2004; accepted June 14, 2004; published October 8, 2004)

High-voltage condensers in a polarity-inversion two-stage Marx surge generator are charged from −40 to −60 kV using a power supply, and the electric charges in the condensers are discharged to an X-ray tube after closing the gap switches in the surge generator using a trigger device. The X-ray tube is a demountable diode, and the turbomolecular pump evacuates air from the tube with a pressure of approximately 1 mPa. Sharp K-series characteristic X-rays of molybdenum are produced without using a monochromatic filter, since the tube utilizes a disk cathode and a rod target, and bremsstrahlung rays are not emitted in the opposite direction to that of electron acceleration. The peak tube voltage increased with increasing charging voltage and increasing space between the target and cathode electrodes. At a charging voltage of −60 kV and a target-cathode space of 1.0 mm, the peak tube voltage and current were 110 kV and 0.75 kA, respectively. The pulse width ranged from 40 to 100 ns, and the maximum dimension of the X-ray source was 3.0 mm in diameter. The number of generator-produced K photons was approximately 7×10^{14} photons/cm^2·s at 0.5 m from the source. [DOI: 10.1143/JJAP.43.7324]

KEYWORDS: flash X-ray, characteristic X-ray, quasi-monochromatic radiography, bremsstrahlung X-ray distribution

1. Introduction

Flash X-ray generators have been developed as a powerful tool in high-speed radiography because they produce extremely short X-ray pulses of less than 1 μs. Currently, most generators utilize a multistage Marx surge generator[1,2] in order to produce high-photon-energy flash X-rays by increasing the maximum tube voltage. On the other hand, soft flash X-ray generators[3–7] with photon energies of less than 150 keV can be applied to biomedicine, and the repetition rate has been increased to the sub-kilohertz order.[8]

High-dose-rate monochromatic X-rays are produced by a synchrotron in conjunction with single crystals and have been applied to X-ray phase imaging[9,10] and microangiography.[11] Subsequently, because extremely high-dose-rate quasi-monochromatic X-rays are produced from the axial direction of weakly ionized linear plasma,[12–14] high-speed biomedical radiography has been performed. However, the bremsstrahlung X-rays are produced using targets of molybdenum, silver, cerium, and tungsten, since high-photon-energy bremsstrahlung X-rays are not absorbed effectively in the linear plasma. In addition, in cases where cold cathode triodes are employed, it is difficult to increase the condenser charging voltage to increase the photon energies of characteristic X-rays due to vacuum breakdown; the target voltage is equal to the charging voltage.

Because bremsstrahlung X-ray intensity varies with changes in the angle and direction of electron acceleration, characteristic X-rays are produced without using a monochromatic filter by selecting the irradiation direction. Although bremsstrahlung intensity is proportional to the atomic number, the angle selection will be a useful technique to produce quasi-monochromatic X-rays.

In this article, we describe a compact flash X-ray generator utilizing a molybdenum-target radiation tube, used to perform a preliminary experiment for generating quasi-monochromatic X-rays using the angle dependence of bremsstrahlung rays.

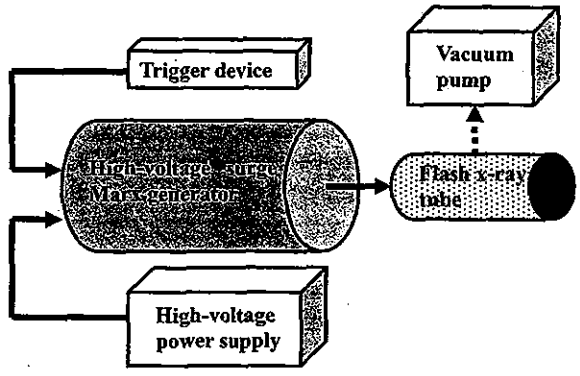

Fig. 1. Block diagram of compact quasi-monochromatic flash X-ray generator.

2. Generator

2.1 *High-voltage circuit*

Figure 1 shows a block diagram of a compact quasi-monochromatic flash X-ray generator. This generator consists of the following components: a constant high-voltage power supply, a polarity-inversion two-stage surge Marx generator with a capacity during main discharge of 425 pF, a trigger device for the surge generator, a turbomolecular pump, and a flash X-ray tube. Since the electric circuit of the surge generator employs a polarity-inversion two-stage Marx line (Fig. 2), the surge produces twice the potential of the condenser charging voltage. When two condensers inside of the surge generator are charged from −40 to

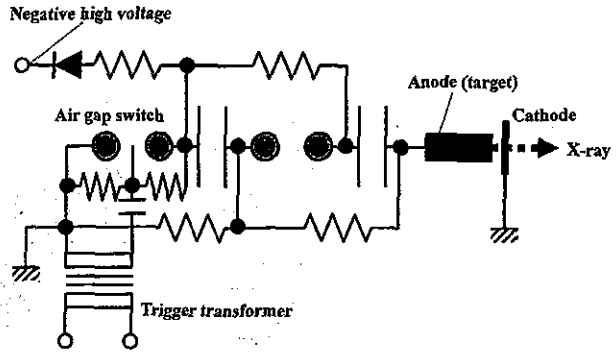

Fig. 2. Circuit diagram of flash X-ray generator.

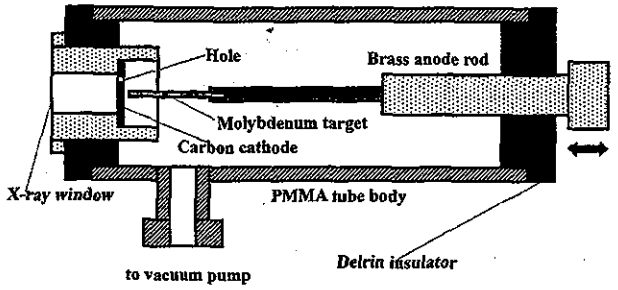

Fig. 3. Schematic drawing of flash X-ray tube.

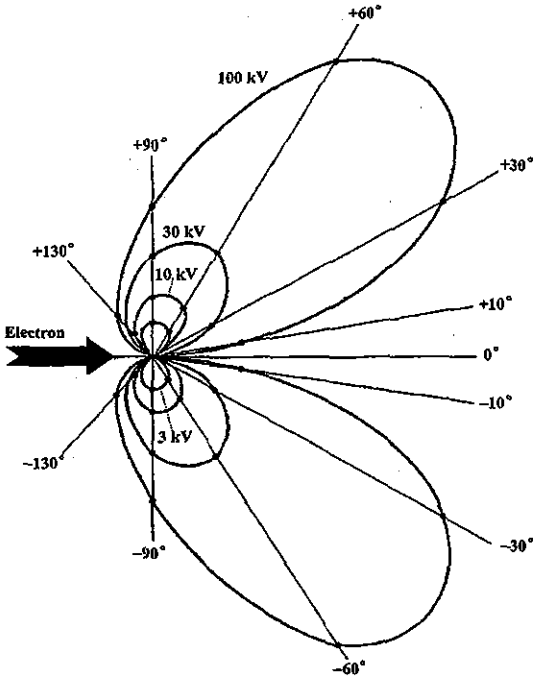

Fig. 4. Bremsstrahlung X-ray intensity distribution vs angle.

−60 kV, the ideal output voltage ranges from 80 to 120 kV.

2.2 *X-ray tube*

The X-ray tube is of the demountable diode type, as illustrated in Fig. 3. This tube is connected to the turbomolecular pump with a pressure of approximately 1 mPa and consists of the following major devices: a rod-shaped molybdenum target, a disk cathode made of graphite, a polyethylene terephthalate (Mylar) X-ray window 0.25 mm in thickness, and a polymethyl methacrylate (PMMA) tube body. The target-cathode (T–C) space was regulated from the outside of the X-ray tube by rotating the anode rod, and the transmission X-rays are obtained through a 1.0 mm-thick graphite cathode and an X-ray window. Because bremsstrahlung rays are not emitted in the opposite direction to that of electron acceleration (Fig. 4), characteristic X-rays can be produced.

3. Characteristics

3.1 *Tube voltage and current*

Tube voltage and current were measured using a high-voltage divider with an input impedance of 10 kΩ and a current transformer, respectively (Figs. 5 and 6). The voltage and current roughly displayed damped oscillations. At a constant T–C space of 1.0 mm, peak voltage increased slightly with increasing charging voltage. In contrast, peak

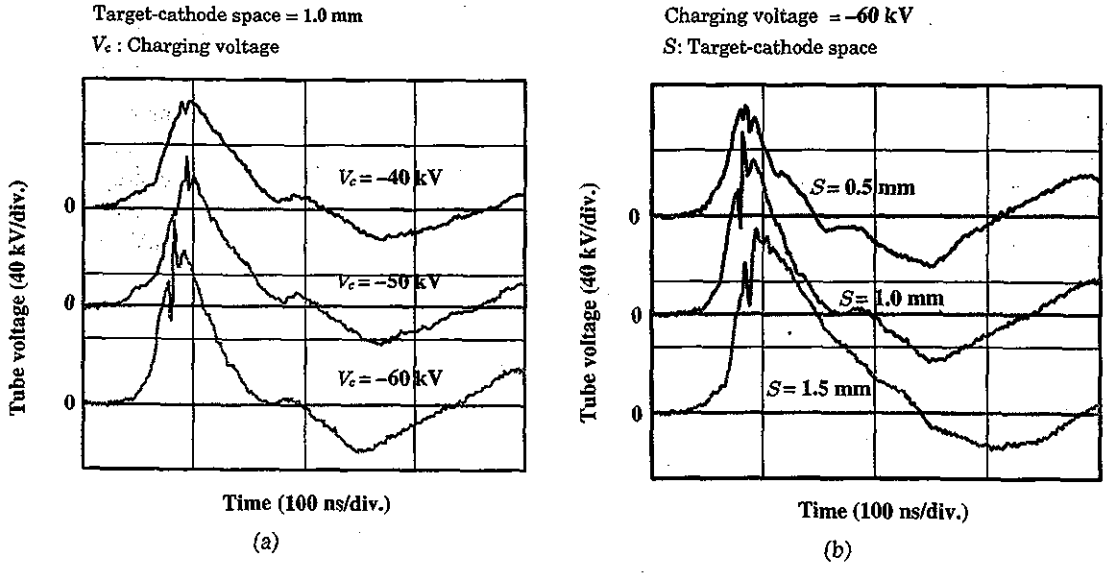

Fig. 5. Variations in tube voltage with changes in (a) charging voltage and (b) space.

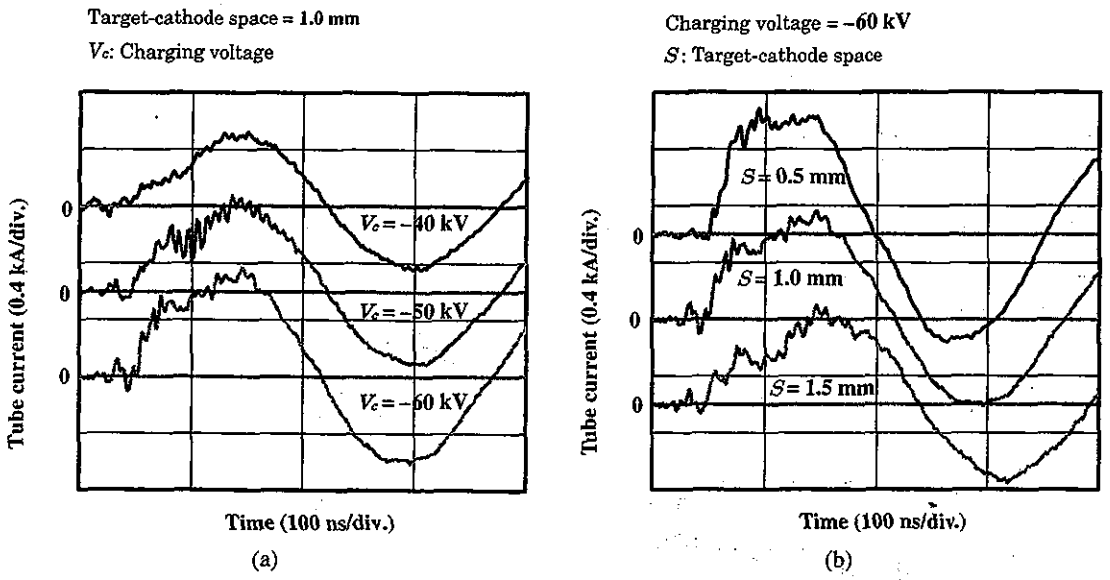

Fig. 6. Tube currents with changes in (a) charging voltage and (b) space.

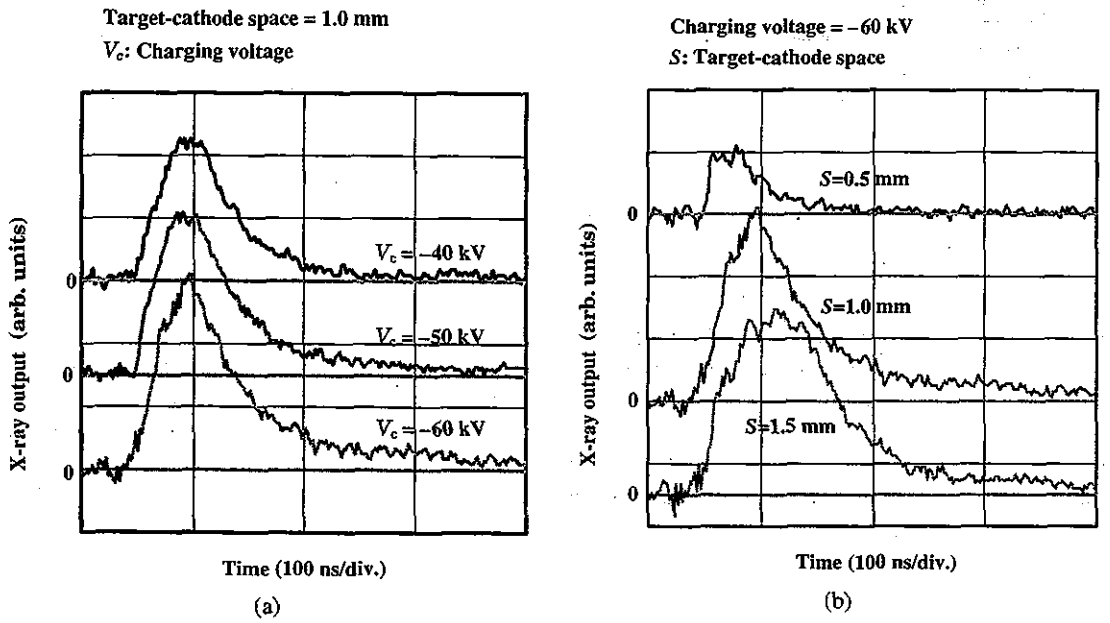

Fig. 7. X-ray outputs according to changes in (a) charging voltage and (b) space.

voltage substantially increased when T–C space was increased at a constant charging voltage of −60 kV. Subsequently, peak tube current increased with increasing charging voltage. When T–C space was increased, current rise time increased, and peak current decreased. At a charging voltage of −60 kV and a T–C space of 1.0 mm, peak tube voltage and current were 110 kV and 0.75 kA, respectively.

3.2 *X-ray output*

X-ray output pulse was detected using a combination of a plastic scintillator and a photomultiplier (Fig. 7). When the charging voltage was increased, the pulse height increased, but the width seldom varied. Next, with increases in the T–C space, the height was maximized, and the width increased. In the present work, the width ranged from 40 to 100 ns. Next, the time-integrated X-ray intensity measured using a thermoluminescence dosimeter (Kyokko TLD Reader 1500 having MSO-S elements without energy compensation) was approximately 3.0 μC/kg at 0.5 m from the X-ray source with a charging voltage of −60 kV and a T–C space of 1.0 mm.

3.3 *X-ray source*

In order to measure the images of the X-ray source, we employed a pinhole camera with a hole diameter of 100 μm (Fig. 8). When the charging voltage was increased, the plasma X-ray source grew, and both spot dimension and intensity increased. The maximum dimension was almost equal to the target diameter and had a value of approximately 3.0 mm.

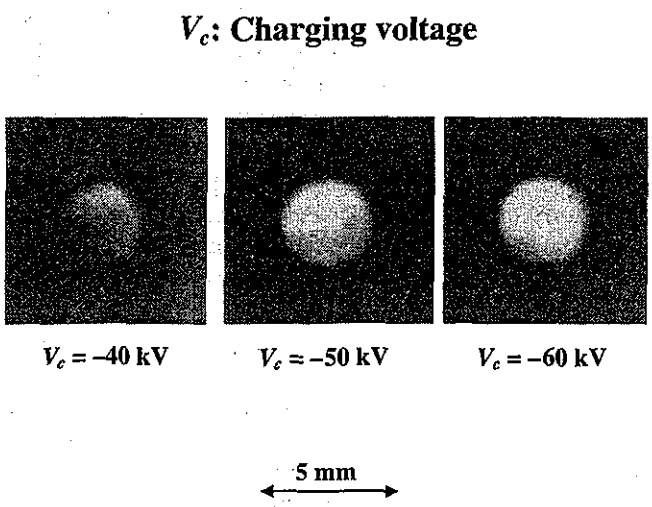

Fig. 8. Images of X-ray source with changes in charging voltage at constant space between target and cathode electrodes.

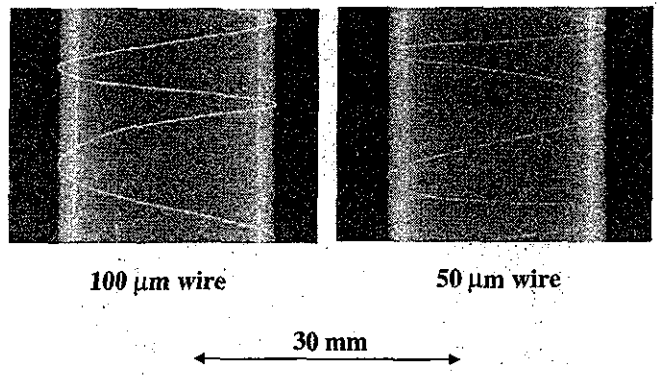

Fig. 10. Radiograms of tungsten wires of 50 and 100 μm in diameter coiled around pipes made of polymethyl methacrylate.

3.4 *X-ray spectra*

X-ray spectra were measured by a transmission-type spectrometer with a lithium fluoride curved crystal 0.5 mm in thickness. The spectra were measured using a computed radiography (CR) system[15] (Konica Regius 150) with a wide dynamic range, and relative X-ray intensity was calculated from Dicom digital data. Figure 9 shows the measured spectra from the molybdenum target. We observed sharp lines of K-series characteristic X-rays, while bremsstrahlung rays were hardly detected. The characteristic X-ray intensity of the Kα and Kβ lines substantially increased with increasing charging voltage.

4. Radiography

Flash radiography was performed using the CR system at 0.5 m from the X-ray source, and the charging voltage and the T–C space were −60 kV and 1.0 mm, respectively.

Firstly, rough measurements of spatial resolution were made using wires. Figure 10 shows radiograms of tungsten wires coiled around a pipe made of polymethyl methacrylate. Although the image contrast increased with increasing wire diameter, a 50-μm-diameter wire could be observed.

An image of plastic bullets falling into a polypropylene beaker from a glass test tube is shown in Fig. 11. Because the X-ray pulse widths were approximately 60 ns, the stop-motion image of bullets could be obtained. Figure 12 shows an angiogram of a rabbit heart; iodine-based microspheres of 15 μm in diameter were used, and fine blood vessels of approximately 100 μm were visible.

5. Discussion

Concerning the spectrum measurement, sharp molybdenum K-series characteristic X-rays were obtained, and monochromatic Kα lines can be obtained using a zirconium filter. The photon energies of characteristic X-rays are determined by the target element, and the X-ray intensity increases with increasing tube voltage by increasing the charging voltage. As compared with the plasma flash X-ray generator utilizing a molybdenum target triode,[13] bremsstrahlung X-rays were hardly observed at all even when higher tube voltages were applied to the diode, since the characteristic X-rays were produced from the target tip. Because the maximum tube voltage can be increased easily, and high-photon-energy K-series characteristic X-rays from

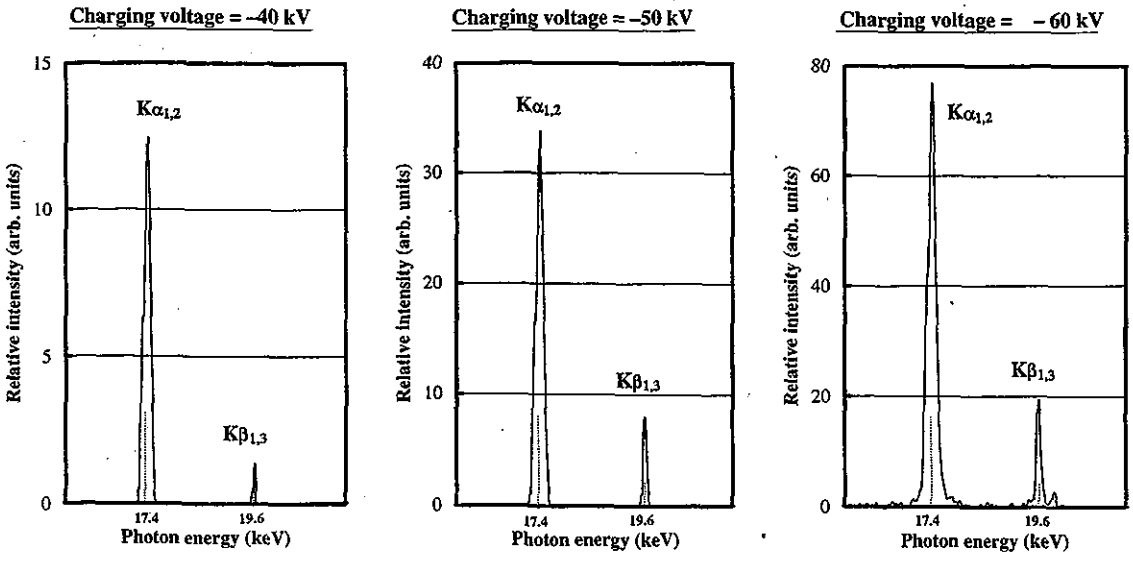

Fig. 9. X-ray spectra from weakly ionized molybdenum plasma according to changes in charging voltage with space of 1.0 mm.

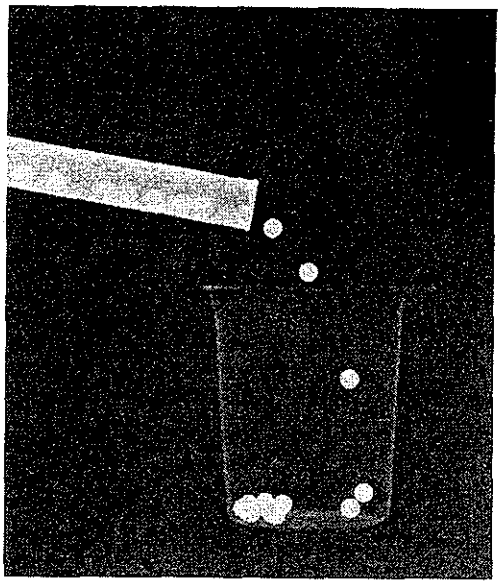

Fig. 11. Radiograms of plastic bullets falling into polypropylene beaker from glass test tube.

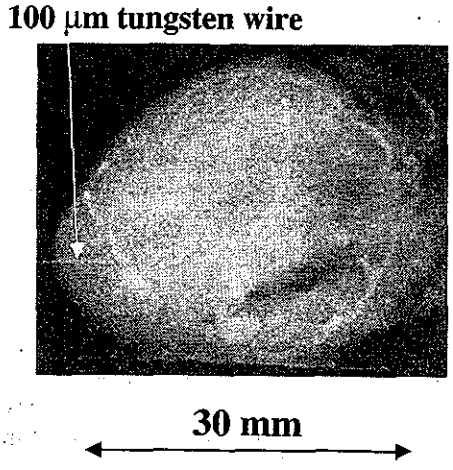

Fig. 12. Angiogram of rabbit heart.

the cerium or tungsten target can be produced. In particular, the cerium target is very useful in order to perform microangiography using iodine-based contrast mediums.

In this research, although the number of generator-produced characteristic K photons was approximately 7×10^{14} photons/cm^2·s at 0.5 m from the source, the number can be increased easily by increasing the electrostatic energy in the condensers.

Using this generator, because the photon energies of characteristic X-rays can be selected, various quasi-monochromatic high-speed radiographies, such as high contrast microangiography and photon-counting radiography for decreasing noise from radiograms, will be possible.

Acknowledgment

This work was supported by Grants-in-Aid for Scientific Research (13470154, 13877114, and 16591222) and Advanced Medical Scientific Research from MECSST, Grants from Keiryo Research Foundation, JST (Test of Fostering Potential), NEDO, and MHLW (HLSRG, RAMT-nano-001, RHGTEFB-genome-005, and RGCD13C-1).

1) A. Mattsson: Physica Scripta **5** (1972) 99.
2) R. Germer: J. Phys. E: Sci. Instrum. **12** (1979) 336.
3) E. Sato, H. Isobe and F. Hoshino: Rev. Sci. Instrum. **57** (1986) 1399.
4) E. Sato, M. Sagae, K. Takahashi, A. Shikoda, T. Oizumi, Y. Hayasi, Y. Tamakawa and T. Yanagisawa: Med. & Biol. Eng. & Comput. **32** (1994) 295.
5) A. Shikoda, E. Sato, M. Sagae, T. Oizumi, Y. Tamakawa and T. Yanagisawa: Rev. Sci. Instrum. **65** (1994) 850.
6) E. Sato, M. Sagae, A. Shikoda, K. Takahashi, T. Oizumi, M. Yamamoto, A. Takabe, K. Sakamaki, Y. Hayasi, H. Ojima, K. Takayama and Y. Tamakawa: Proc. SPIE **2869** (1996) 937.
7) K. Takahashi, E. Sato, M. Sagae, T. Oizumi, Y. Tamakawa and T. Yanagisawa: Jpn. J. Appl. Phys. **33** (1994) 4146.
8) E. Sato, K. Takahashi, M. Sagae, S. Kimura, T. Oizumi, Y. Hayasi, Y. Tamakawa and T. Yanagisawa: Med. & Biol. Eng. & Comput. **32** (1994) 289.
9) T. J. Davis, D. Gao, T. E. Gureyev, A. W. Stevenson and S. W. Wilkins: Nature **373** (1995) 595.
10) A. Momose, T. Takeda, Y. Itai and K. Hirano: Nature Medicine **2** (1996) 473.
11) H. Mori *et al.*: Radiology **201** (1996) 173.
12) E. Sato, Y. Hayasi, R. Germer, E. Tanaka, H. Mori, T. Kawai, H. Obara, T. Ichimaru, K. Takayama and H. Ido: Jpn. J. Med. Imag. Inform. Sci. **20** (2003) 148.
13) E. Sato, Y. Hayasi, R. Germer, E. Tanaka, H. Mori, T. Kawai, H. Obara, T. Ichimaru, K. Takayama and H. Ido: Jpn. J. Med. Phys. **23** (2003) 123.
14) E. Sato, Y. Hayasi, R. Germer, E. Tanaka, H. Mori, T. Kawai, T. Ichimaru, K. Takayama and Hideaki Ido: Rev. Sci. Instrum. **74** (2003) 5236.
15) E. Sato, K. Sato and Y. Tamakawa: Ann. Rep. Iwate Med. Univ. Sch. Lib. Arts and Sci. **35** (2000) 13.

研　究　論　文

Monochromatic polycapillary imaging utilizing a computed radiography system

Michiaki Sagae[1)*], Eiichi Sato[1)], Yasuomi Hayasi[1)], Etsuro Tanaka[2)], Hidezo Mori[3)], Toshiaki Kawai[4)], Haruo Obara[5)], Toshio Ichimaru[6)], Kazuyoshi Takayama[7)], Hideaki Ido[8)]

[1)] *Department of Physics, Iwate Medical University*
[2)] *Department of Nutritional Science, Faculty of Applied Bio-science, Tokyo University of Agriculture*
[3)] *Department of Cardiac Physiology, National Cardiovascular Center Research Institute*
[4)] *Electron Tube Division #2, Hamamatsu Photonics Inc.*
[5)] *Department of Radiological Technology, College of Medical Science, Tohoku University*
[6)] *Department of Radiological Technology, School of Health Sciences, Hirosaki University*
[7)] *Shock Wave Research Center, Institute of Fluid Science, Tohoku University*
[8)] *Department of Applied Physics and Informatics, Faculty of Engineering, Tohoku Gakuin University*

Research Code No.: 200, 204.1
Key Words: monochromatic radiography, quasi-parallel radiography, x-ray lens, polycapillary plate

Abstract

A fundamental study on quasi-parallel radiography using a polycapillary plate and a copper-target x-ray tube is described. In the experiments, the tube voltage was regulated from 12 to 22 kV, and the tube current was regulated within 3.0 mA by the filament temperature. The exposure time was controlled in order to obtain optimum x-ray intensity, and the maximum focal spot dimensions were approximately 2.0 × 1.5 mm. The thickness and the inner capillary tube diameter of the polycapillary were 1.0 mm and 25 μm, respectively. Monochromatic x-rays were produced using a 10 μm-thick nickel filter with a tube voltage of 17 kV, and these rays were formed into quasi-parallel beams by the polycapillary. The radiogram was taken using a computed

* 岩手医科大学教養部物理学科〔〒020-0015 岩手県盛岡市本町通3-16-1〕: Department of Physics, Iwate Medical University
e-mail: msagae@iwate-med.ac.jp

radiography system utilizing imaging plates. In the measurement of image resolution, the spatial resolution hardly varied according to increases in the distance between the resolution-test chart and imaging plate using a polycapillary. A 50 μm tungsten wire could be observed, and fine blood vessels of approximately 100 μm were visible in angiography.

Received Jan. 7, 2004; revision accepted Jul. 5, 2004

1. Introduction

Monochromatic parallel radiography typically utilizes a synchrotron in conjunction with silicon single crystals and it has been applied in x-ray phase imaging[1-3]. It has also been applied in high contrast micro-angiography[4-7] because x-rays with energies of approximately 35 keV are absorbed effectively by the iodine-based contrast medium.

In order to produce monochromatic x-rays without using the synchrotron, we developed a molybdenum x-ray tube[8] with a transmission-type molybdenum target, which is used as a monochromatic filter for absorbing bremsstrahlung x-rays. In addition, from weakly ionized linear plasma, we found irradiations of intense and sharp characteristic x-rays[9-12].

Recently, several different x-ray lenses[13,14] have been developed, and a polycapillary plate[8-15] has been shown to be useful to perform quasi-parallel radiography with lower photon energy. For this, the plate thickness is about 1 mm, and it is very difficult to design a thicker plate due to technical limitation for increasing the strait capillary length.

In biomedical radiography, because the image processing can be done easily with a Computed Radiography (CR) system[16,17] utilizing imaging plates, the CR system is useful for monochromatic parallel radiography, regardless of whether the image resolution falls as compared with an x-ray film; the spatial resolution is primarily determined by the minimum sampling pitch of 87.5 μm.

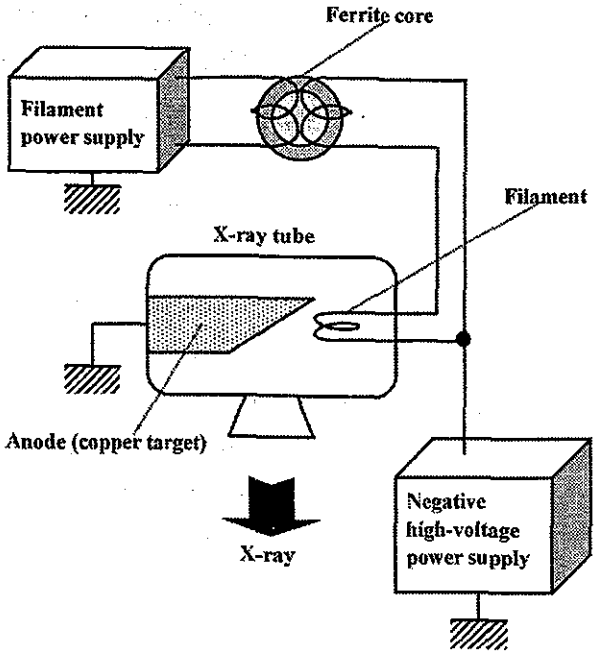

Fig. 1. Circuit diagram of the x-ray generator.

In this article, we describe a monochromatic quasi-parallel radiography system utilizing a polycapillary plate with an inner capilliary diameter of 25 μm, a CR system, and a copper-target radiation tube to realize a low-priced x-ray system utilizing an x-ray lens.

2. Experimental setup

Figure 1 shows the circuit diagram of the x-ray generator, which consists of a negative high-voltage power supply, a filament (hot cathode) power supply, and a copper-target x-ray tube. The negative high voltage is applied to the cathode electrode, and the anode (target) is connected to the ground. In the experiments, the

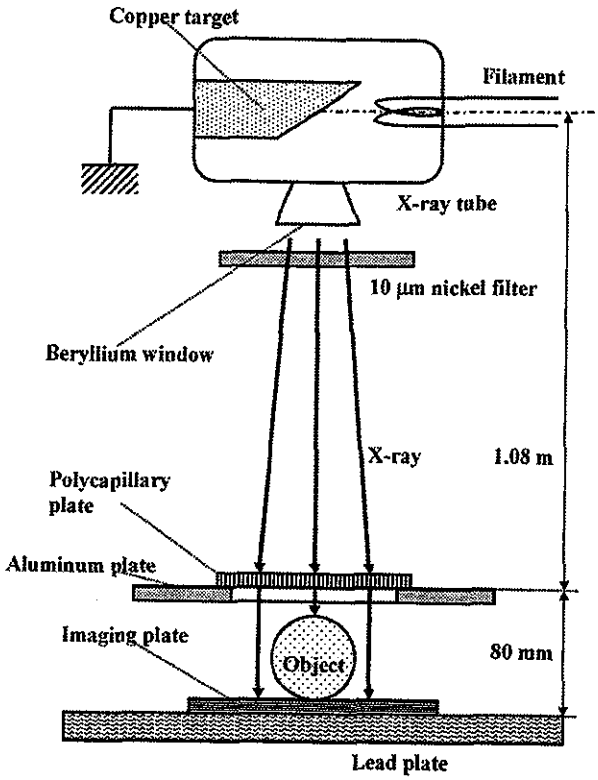

Fig. 2. Experimental setup for polycapillary imaging utilizing a CR system.

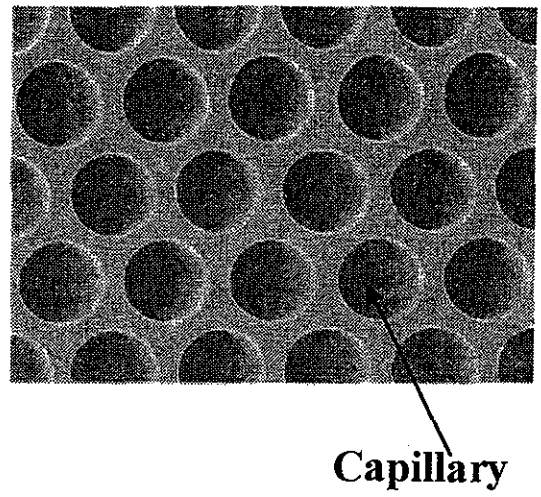

Fig. 3. Polycapillary plate.

tube voltage was regulated from 12 to 22 kV, and the tube current was regulated by the filament temperature and ranged from 1.0 to 3.0 mA. The exposure time was controlled in order to obtain optimum x-ray intensity.

The experimental setup for performing polycapillary imaging is shown in Fig. 2. Monochromatic x-rays were produced using a 10 μm-thick nickel filter, and these rays were formed into quasi-parallel beams by a polycapillary plate (Fig. 3). The polycapillary plate was J5022-21 (Hamamatsu Photonics Inc.), and the plate thickness was 1.0 mm. The outer, effective, and inner capilliary diameters were 87 mm, 77 mm, and 25 μm, respectively. Radiography was performed by a CR system (Konica Regius 150) utilizing imaging plates. The distance between the x-ray source and the polycapillary was 1.08 m, and the polycapillary plate was set on an aluminum plate. The distance between the polycapillary and imaging plates was regulated by the height (30 mm) of the polymethyl methacrylate (PMMA) spacers used.

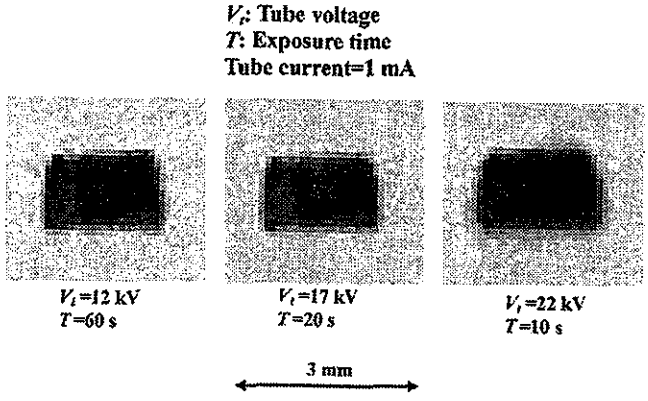

Fig. 4. Images of the x-ray source measured using a 50 μm-diameter pinhole while changing the tube voltage.

3. Characteristics

3.1. Focal spot

In order to measure images of the x-ray source, we employed the CR system, a pinhole camera with a hole diameter of 50 μm, and a filter (Fig. 4). When the tube voltage was increased, the focal spot intensity increased; spot dimensions also increased slightly and were approximately 2.0 × 1.5 mm.

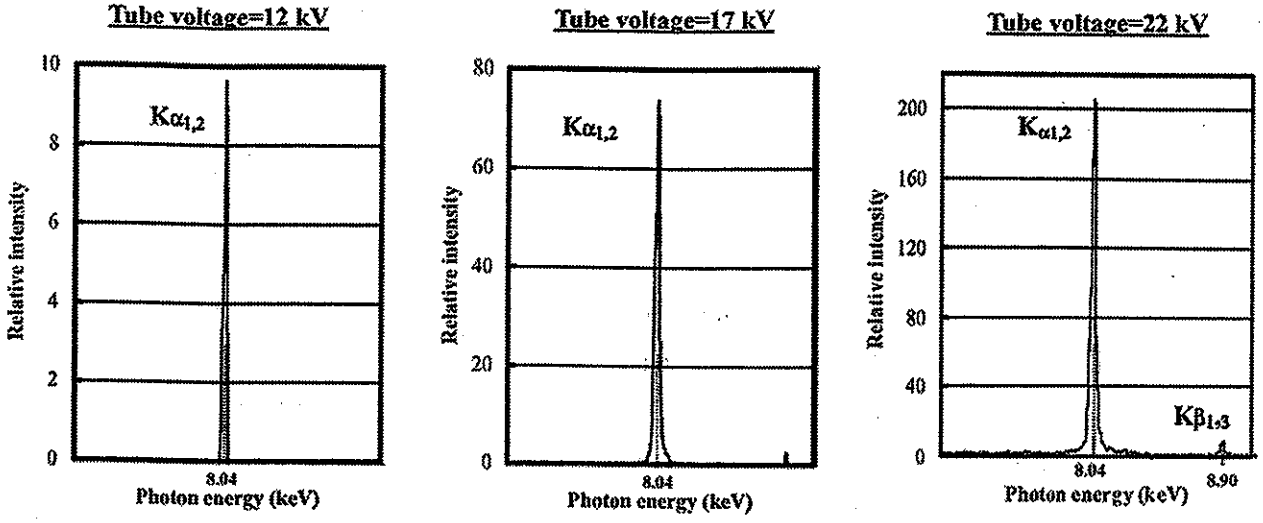

Fig. 5. Measured x-ray spectra while changing the tube voltage.

3.2. *X-ray spectra*

Monochromatic x-ray spectra from the copper-target tube were measured by a transmission-type spectrometer with a lithium fluoride curved crystal 0.5 mm in thickness. The spectra were taken by the CR system with a wide dynamic range, and relative x-ray intensity was calculated from Dicom digital data. Fig. 5 shows measured spectra from the copper target. When the tube voltage was increased, the characteristic x-ray intensity of Kα lines increased.

4. Radiography

The monochromatic radiography was performed with a tube voltage of 17 kV using the filter. Figure 6 shows radiography for imaging a polycapillary plate, and radiograms of the polycapillary are shown in Fig. 7. The center of the black spot in the polycapillary radiogram was mainly imaged by direct transmission beams through capillary holes. As shown in this figure, the spot dimensions increased slightly according to decreases in the PMMA spacer height.

Radiography for imaging a test chart for determining image resolution, and the radio-

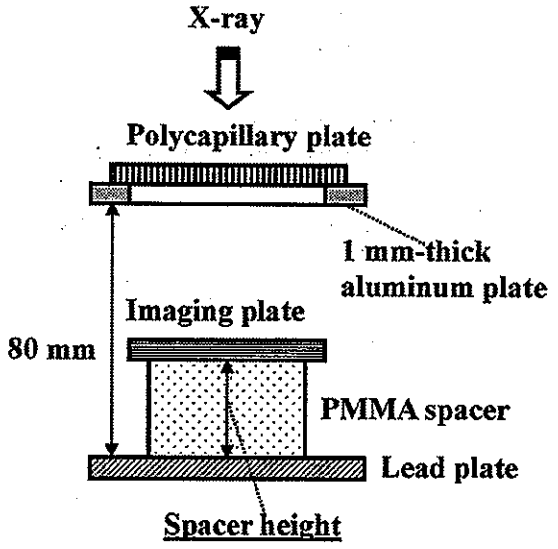

Fig. 6. Radiography for imaging a polycapillary plate while changing the distance between the polycapillary and imaging plates using PMMA spacers.

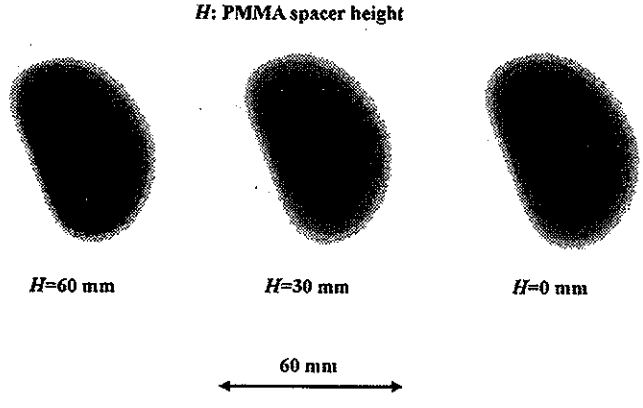

Fig. 7. Radiograms of a polycapillary plate while changing the PMMA height.

grams of 166 μm width lead lines, are shown in Figs. 8 and 9, respectively. Both the image resolution and the line contrast fell with decreases in the spacer height. Figure 10 shows the polycapillary radiography for imaging the test chart; the polycapillary was set on the aluminum plate. With this radiography system, we obtained higher contrast lines as compared with those in Fig. 9. When the spacer height was increased, the image resolution hardly varied, and the image dimensions decreased slightly (Fig. 11).

Figures 12 and 13 show radiography and the radiogram of tungsten wires on a PMMA box, respectively. Although the image contrast increased with increases in the wire diameter, a 50 μm-diameter wire could be observed. The angiography for a rabbit heart is shown in Fig 14; iodine-based microspheres of 15 μm diameter were used, and fine blood vessels of about 100 μm were visible (Fig. 15).

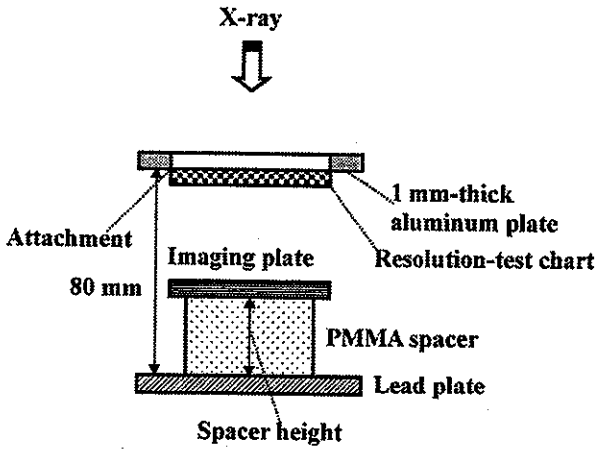

Fig. 8. Radiography for imaging a test chart according to the PMMA spacer height.

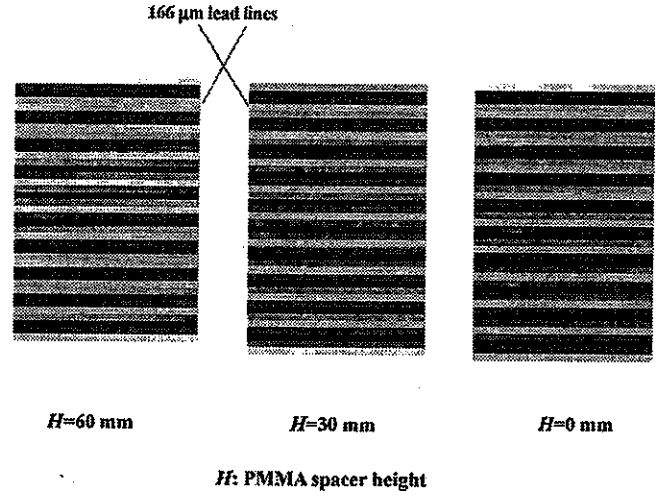

Fig. 9. Radiograms of a test chart according to the PMMA height.

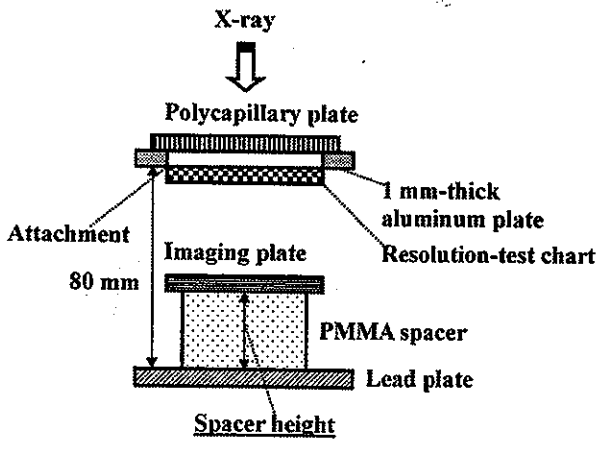

Fig. 10. Radiography for imaging a test chart using a polycapillary plate according to the PMMA height.

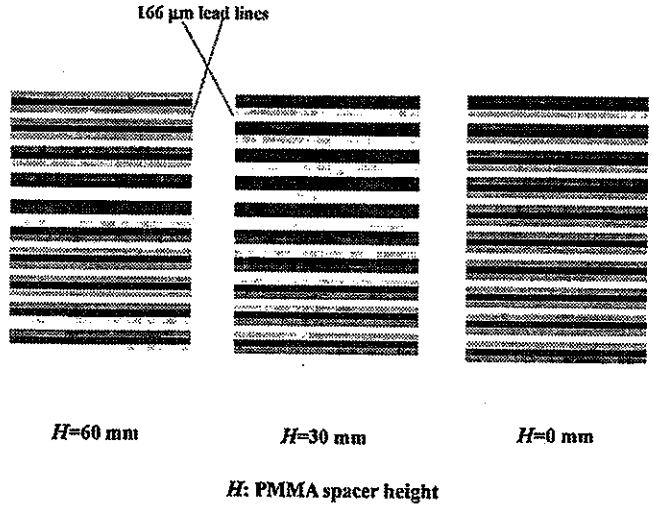

Fig. 11. Radiograms of a test chart using the polycapillary plate according to the PMMA height